Anomaly Localization in Optical Transmissions Based on Receiver DSP and Artificial Neural Network

Huazhi Lun, Xiaomin Liu, Meng Cai, MengFan Fu, Yiwen Wu, Lilin Yi, Weisheng Hu and Qunbi Zhuge*
State Key Laboratory of Advanced Optical Communication Systems and Networks,
Department of Electronic Engineering, Shanghai Jiao Tong University, Shanghai, 200240, China
**Corresponding author: qunbi.zhuge@sjtu.edu.cn*

Abstract: We propose a receiver DSP based scheme to localize WSS anomaly in an optical link. Through extensive simulations, we show that the accuracy reaches up to 96.4% with a good generalization performance. © 2020 The Author(s)
OCIS codes: (060.2330) Fiber optics communications, (060.4510) Optical communications

1. Introduction

The rapid progress of 5G, Internet of things (IoT), cloud computing and high definition online videos have raised high requirements for optical network's flexibility, capacity and efficiency. To fulfill these requirements, the architecture of the optical network needs to be more dynamic and elastic. The widely deployed wavelength selective switch (WSS) in optical links and the design of low margin optical network [1] provide the needed dynamicity, flexibility and high spectral efficiency. However, new issues have also emerged. In particular, the established connections may be interrupted due to the anomaly of deployed WSS. Therefore, to ensure the quality of the communication, it is important to quickly localize the irregular WSS once it occurs. However, few researches have been conducted on this problem. Many relevant works mainly focus on the failure detection [2] and identification [3]. Besides, in some previous works [2], additional devices such as optical spectrum analyzer (OSA) are used, which increases the cost. Thanks to the capability of optical performance monitoring (OPM) provided by coherent receivers, it is possible to build the anomaly localization in a more cost-efficient way.

In this paper, we propose a novel anomaly localization algorithm based on receiver DSP and artificial neural network (ANN). We monitor the power spectrum density (PSD) of received signals and the tap coefficients of the adaptive filter to get the location of the irregular WSS in the fiber link. Compared with [2], the information we used can be easily obtained from receiver DSP and no additional devices such as OSA are needed, leading to a low-cost implementation. In this paper, we explore two types of WSS anomalies: filter shift (FS) and filter tightening (FT). To validate the proposed scheme, we perform extensive simulations and demonstrate its high accuracy, scalability and superior generalization performance.

2. Principles

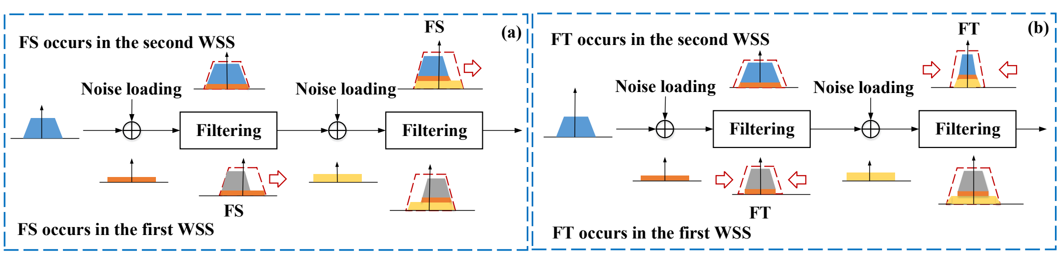

Fig. 1. Illustration of (a) FS anomaly and (b) FT anomaly.

To localize the irregular WSS, it is important to obtain the information about the status of the fiber link. Such information can be obtained through optical signal spectrums using an OSA as described in [2] at the expense of additional hardware cost. Alternatively, we can measure the power spectrum density (PSD) of received signals using fast Fourier transform (FFT) in a coherent receiver. Fig. 1(a) shows the signal PSD when the FS occurs in different locations of the fiber link. To explain the principle, we take a link that consists of two WSS for example. As shown in Fig. 1(a), if the FS occurs in the first WSS, when it passes through the second WSS, the amplifier spontaneous emission (ASE) noise added to the edge part of the PSD will not be filtered. If the FS occurs in the second WSS, however, the ASE added to the edge of the PSD will be filtered in both the first and the second WSS's. The principle for the FT anomaly is similarly illustrated in Fig. 1(b). Consequently, when the anomaly location is different, the interaction between the ASE and the filtering effect of the WSS is also different. As a result, such differences are reflected in the PSD, the auto-correlation function (ACF) of the received signal, and the converged tap coefficients in the adaptive filter since the inter-symbol-interference (ISI) caused by WSS is different. Therefore, the localization problem can be addressed by analyzing these characteristics.

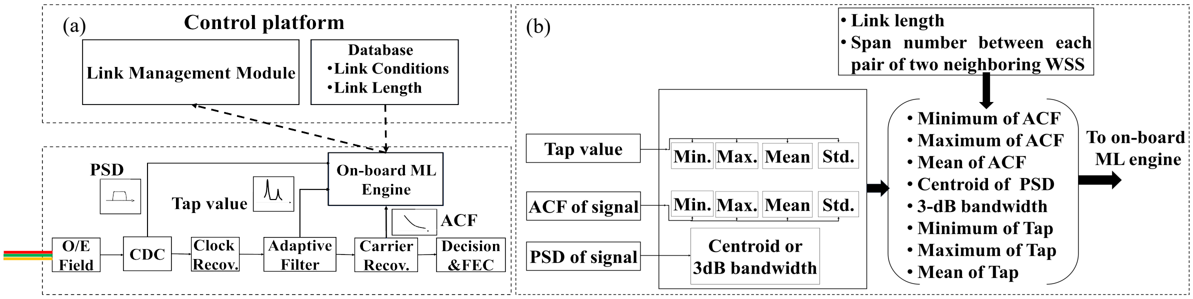

Fig. 2. (a). The architecture of the proposed algorithm. (b). The pre-processing of the feature

The proposed anomaly localization scheme is described in Fig. 2(a). The PSD, tap coefficients and ACF are extracted from the chromatic dispersion compensator (CDC) module, the adaptive filter and the carrier phase recovery module in the coherent receiver, respectively. An ANN is adopted, and it can be embedded in the on-board machine learning (ML) engine as described in [6] to provide fast localization processing. As shown in Fig. 2(b), the PSD and the tap coefficients are pre-processed before being used as the features to the ANN. The centroid of the PSD is calculated using $f_{centroid} = \int_{-\infty}^{+\infty} f * PSD(f)df \,/\left(\int_{-\infty}^{+\infty} PSD(f)df\right)$ [4]. In addition, the 3-dB bandwidth of the PSD is also calculated. The minimum value, maximum value, average value, standard deviation of the tap coefficients and the ACF of the symbols after carrier phase recovery are calculated. Then all these features together with the span number between every two neighboring WSS's and the total link length are input to the on-board ML engine to perform anomaly localization. The final output of the ANN is then sent to the link management module and then proper actions can be taken to recover the optical link.

3. Simulation and results

3.1. Simulation Setup

The simulation setup is depicted in Fig. 3. The length of the fiber link is randomly chosen from 800km to 1200km with a fixed span length of 80km, and five WSS's are distributed randomly in the link. The link length and the WSS location distributions are referred to as link configurations in the following discussions. To simulate the nonlinear impairments of the fiber, the split-step Fourier method (SSFM) with a step size of 20 m [5] is employed. At the end of each span, the loss of the fiber is fully compensated by an Erbium-doped fiber amplifier (EDFA) and the noise figure is 5dB. In our simulation, a single channel scenario is considered due to the slow simulation speed of the SSFM for wavelength division multiplexing (WDM) transmissions. The results should be applicable to WDM systems, because the WSS filtering is applied to each WDM channel independently. At the transmitter side, 35Gbaud PDM-16QAM symbols are generated and then pulse shaped by a root-raised-cosine (RRC) filter with a roll-off factor of 0.02. At the receiver side, after CDC, a matched filter is applied followed by a least-mean-square (LMS) based adaptive filter and a phase-locked loop (PLL). The adopted architecture of the ANN consists of one input layer with 16 neurons and two hidden layers with 25 neurons for each. The neuron number of the output layer is 5, corresponding to the location of five WSS's in the link.

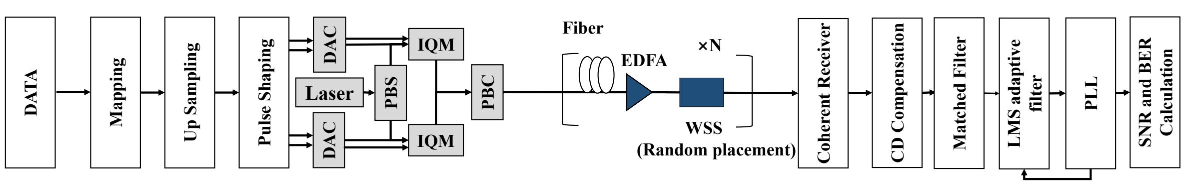

Fig. 3. Simulation setup.

To train the ANN, 1200 data samples are generated under 120 different link configurations. For each data sample, we first randomly choose a link configuration and then randomly choose a shift value or bandwidth value from 14GHz to 19GHz and 20GHz to 24GHz, respectively. Finally, 70% of the dataset is randomly selected for training and the left is for testing.

To test the generalization performance of the proposed algorithm in different scenarios, we generate additional data samples modulated using PDM-QPSK, PDM-8QAM and PDM-32QAM. For each modulation format, the sample size is 225, and the distances are 640km, 800km and 1120km. To generate them, we randomly choose a distribution of WSS, and then either sweep the FS value from 14GHz to 19GHz with a step size of 0.2GHz or sweep the FT value from 20GHz to 24 GHz with a step size of 0.2GHz. These data samples are never seen by the ANN, and thus they can be used to test the generalization performance of the proposed scheme.

Another important scenario is that the anomalies of multiple WSS's might occur simultaneously. We test our scheme in this scenario assuming two WSS's are abnormal. For the FS, we first choose a 1200km link with PDM-16QAM, and then set the FS of the fourth WSS to 16GHz when sweeping the FS of the third WSS from 15.5GHz to 19GHz with a step size of 0.05GHz. For the FT, we set the bandwidth of the fourth WSS to 23GHz and sweep the bandwidth of the third WSS from 21.5 GHz to 25GHz with a step size of 0.05GHz.

3.2. Results

We first plot the learning curve of the proposed scheme in Fig. 4(a). The result illustrates that the algorithm has converged, and no overfitting occurs. In Fig. 4(b), the accuracy of the algorithm is shown, and the final accuracy reaches 96.4%. We believe the accuracy can be further improved by fine-tuning the architecture of the ANN, and this will be left for future study. We then try to use the principle components analysis (PCA) to reduce the computation burden and the storage requirements of the on-board ML engine. In Fig. 4(c), we plot the accuracy as a function of the preserved features. Note that originally we have in total 16 features. It can be seen from the figure, when the preserved number of features is 8, the accuracy can achieve 91.2%, and when the preserved number is 10, the accuracy can achieve 95%. In practice, the trade-off between complexity and performance should be made according to practical needs.

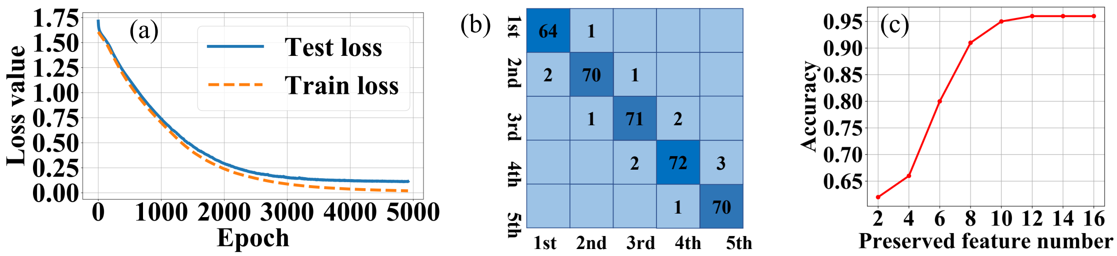

Fig. 4. (a) The loss curves of training and testing. (b) The confusion matrix. The horizontal axis represents the actual location, and the vertical axis represents the estimated location. (c) The accuracy for different preserved number of features.

We then test the performance when the trained ANN is applied to the PDM-QPSK, PDM-8QAM, and PDM-32QAM with transmission distances of 640km,800km and 1120km. All these data samples are never be used in the previous training phase and testing phase. The results are summarized in Table 1, and high accuracy is also achieved, which indicating the good generalization performance of the proposed scheme.

Table 1. The accuracy of the proposed scheme in new scenarios.

Modulation Format	QPSK	8QAM	32QAM
640km (case I/case II)	91.9%	92.7%	91.4%
800km (case I/case II)	94.1%	95.9%	91.9%
1120km (case I/case II)	95.7%	95.1%	95.2%

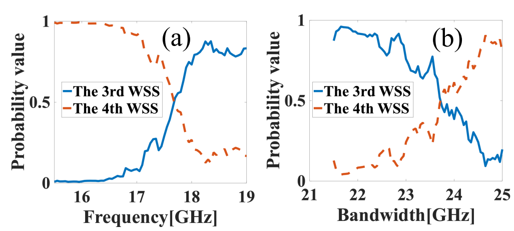

Fig. 5. Probability of the softmax layer for (a) different FS value; (b) different FT value.

Finally, we test the performance of the proposed scheme when multiple WSS's are abnormal. The probability information of the softmax layer is used as described in [3]. Fig. 5(a) plots the result of the FS case. At first, the fourth WSS has a greater impact on the system than the third one. So, the probability of the fourth WSS is higher than the third one. As the FS value of the third WSS increases, the probability of it gradually exceeds the fourth. Similar result has been observed in the FT case as shown in Fig. 5(b). The results above demonstrate the proposed scheme can be extended to the case when multiple WSS's are abnormal.

4. Conclusion

A WSS anomaly localization algorithm based on receiver DSP and ANN is proposed. We demonstrate its performance in terms of accuracy, scalability and generalization through extensive simulations in various scenarios. The accuracy is above 90% for most of the cases, indicating its high effectiveness in localizing the WSS anomaly.

This work was supported by NSFC (61801291), Shanghai Rising-Star Program (19QA1404600) and National Key R&D Program of China (2018YFB1801203).

[1]. Y. Pointurier, et.al., J. Opt. Commun. Netw. 9(1), A9 (2017).
[2]. B. Shariati, et.al., J. Light. Technol. 37(2), 433–440 (2019).
[3]. H. Lun, et.al., in ECOC, P104(2019).
[4]. C. Delezoide, el.al., in OFC, Th2A.48(2019).
[5]. Q. Zhuge, et.al., J. Light. Technol. 37, 3055-3063 (2019).
[6]. Y. Zhao, et.al. J. Opt. Commun. Netw. 12(1), A49-A57 (2020).